A novel reactive magnetron sputtering technique for producing insulating oxides of metal alloys and other compound thin films

I. Safi*

Department of Physics, Loughborough University, Loughborough, LE11 3TU, UK

Abstract

Problems associated with reactive magnetron sputtering from elemental (i.e. non-compound) targets have been successfully solved in this work. The elements of this achievement are: (i) the use of mid-frequency (i.e. 40 kHz) AC power in the floating mode, between two magnetrons, allowed the reactive sputtering process to be arc-free and hence eliminating the undesired effects of arcing in reactive sputtering such as driving the process to become unstable, creating defects in the films and reducing the target lifetime. (ii) The combination of DC and mid-frequency AC power in a novel way using a filter to protect the DC power supply from the AC one (or the independently DC powered magnetrons method) permitted the composition of the produced films to be easily and independently manipulated by varying the magnitude of power applied to each magnetron. (iii) The use of very fast feedback methods to automatically control the admission rate of oxygen into the sputtering chamber (i.e. plasma emission monitoring or voltage control) allowed the stoichiometry of the deposited films to be independently controlled. This also allowed the deposition rate of the sputtered films to be high. (iv) Sputtering from two magnetrons made the production of alloys or multi-element compounds, which are either difficult or impossible to be formed from single targets, an easy task. (v) Substrate rotation enhanced atomic level mixing of the film constituents. The stoichiometry of the film was controlled by plasma emission monitoring or voltage control on one magnetron, and dopants were added by sputtering from the other magnetron. This means that the former magnetron served two purposes; the first was to sputter metal and oxidise it, and the second purpose was to oxidise the metal sputtered from the other magnetron. This novel technique opens the door wide for investigating virtually all potentially promising thin oxide films. Using this technique, a large range of alloy-oxide films was deposited at high rates. In fact, the independent control of both the metallic composition and stoichiometry was very valuable in identifying the optimum properties of these films. That is, giving transparent films of different refractive indices for optical applications. Furthermore, such a technique may also be capable of investigating other types of thin films (e.g. hard coatings, semiconducting films, superconducting films, etc.). © 2000 Elsevier Science B.V. All rights reserved.

Keywords: Thin film; Oxide; Reactive sputtering; Two magnetrons; AC and DC technique; PEM; Voltage control; Composition; Stoichiometry; Arcing

*Corresponding address. P.O. Box 4470, Damascus, Syria. Tel.: +963-11-5117808.

1. Introduction

Reactive sputtering, where a metal target is sputtered by an inert gas (e.g. argon) in the presence of a reactive gas (e.g. oxygen), to produce a film of electrically insulating material has proved to be difficult to introduce as an industrial process. The simple concept is that metal is sputtered from the target and is incident on the substrate/growing-film-surface, together with reactive gas from the residual atmosphere, to form a compound. The reaction occurs when these species meet on the surface. Energy is provided from the substrate temperature, the high energy of sputtered material or by ions used to bombard the surface. Magnetron sputtering has allowed the sputtering to be undertaken at sufficiently low pressures such that the mean free path for sputtered material is greater than the target-to-substrate distance and the energy of this material and the efficiency of its transfer from the target can be maintained. The magnetron can also be arranged, through unbalancing the magnetic field, and/or operating it in a system to create a closed field, to direct a dense plasma to the surface of the growing film. This plasma can cause an insulating or isolated surface to acquire a floating bias, which leads to it being bombarded with low energy argon ions, to provide energy for excitation energies for chemical and structural reactions. The growth of the film can be controlled in this manner and it does not require the film or substrate to be electrically conducting. If additional bias is required, RF can be used. The problems, which have to be solved, occur at the cathode surface.

The presence of reactive gas in a region of high energy and freshly exposed metal surfaces, which is the sputtering race-track of the magnetron, leads to rapid reaction. If the surface reacts faster than it sputters, a surface compound film is formed, which in general sputters at a much lower rate than the metal, a process which has become to be called 'poisoning'. The transition between metal sputtering and 'poisoning' is dependent upon the power used to sputter and the partial pressure of the reactive gas and occurs at a different level when approached from the metal or 'poisoned' condition. This process leads to a hysteresis being seen between the sputtering parameters and the flow of reactive gas into the chamber and there is a region of this flow where the process is unstable. It becomes one of the rapid deposition of a partially reacted metal or the slow deposition from a poisoned target of a fully reacted film. This problem can be solved by controlling the state of the sputtering surface, and hence the partial pressure of the reactive gas, through the light emitted by the sputtering metal or other gases in the discharge, or in some cases, from the voltage of the sputtering cathode. These techniques provide a fast feedback to the control of the flow of the gas. However,

great care has to be taken with the time constants associated with the changes of gas pressure in a vacuum chamber.

A further solution lies in separating the deposition and reactive process in a cyclic process where a thin metal film is deposited and then converted. In our versions of this process, the substrate is moved (successive plasma anodisation, or SPA) or the magnetron is made to change function from a provider of sputtered metal to one of oxygen and energetic argon ions (successive pulsed plasma anodisation, or SPPA). In both cases, the unbalanced magnetron, the provider of argon-ion energy, is required to operate in the presence of a partial pressure of oxygen.

When the reaction product is insulating and the power is DC, other problems appear. A region of the target-cathode remains covered with reaction product, the racetrack region only can be balanced to be sputtering metal faster than it is reacting with the proportion of reactive gas in the system. This insulating region is subject to bombardment of ions and becomes highly charged, due to charge accumulation or through secondary-electron emission. This leads to rapid localised discharges, arcs, which disrupt the sputtering discharge and causes arc-evaporation from regions of the target, with particle 'spitting' and consequent contamination of the film. If the process is not properly designed, and carefully balanced, an insulating film may be formed on the anode of the discharge and on the chamber walls to give a discharge which changes character with time. These problems can be overcome by using RF in reactive sputtering and target biasing. RF introduces its own problems and is not suitable for the high-rate, large-area processes that are required.

More recently, a solution to these problems has appeared. The insulating surface has to be discharged before the charge accumulates to an extent where an arc is formed. This has been done by providing a reverse potential pulse to the surface within the charge accumulation time. This can be a short pulse applied to a DC supply or AC power applied between two cathodes. The frequency required turns out to be approximately 40 kHz, which can be provided, without the tuning systems necessary with RF, and at low cost. The latter process has the further advantage of creating a continuously cleaned anode, because for the other half of the cycle it is the sputtering cathode. This emerging technique has been utilised recently by a few workers [1–10]. The results were very promising. For example, Szczyrbowski and Braatz [7] have reactively deposited films of SiO_2 at high rates using 40 kHz-AC power applied between two Si magnetrons. In addition to the excellent optical and mechanical properties of the deposited films, no arcing was observed during the entire lifetime of the target, which was more than a week. Schiller et al. [11] have reactively deposited films of

Al_2O_3 from two Al magnetrons using an AC power at different frequencies ranged from 50 Hz to 164 kHz. They reported a significant decrease in the defect density of the deposited films with increasing frequency. The curve, for non-absorbing films, saturated at frequencies greater than 50 kHz, which was an indication of an arc-free process beyond this frequency. They also reported a deposition rate of approximately 60% of that of metallic Al. The rate was almost independent of the frequency in the range they investigated. Scherer et al. [9] have also adopted the two cathodes technique to reactively deposit films of Al_2O_3, SiO_2 and Si_3N_4 using 40 kHz-AC power. They reported deposition rates comparable to those obtained with the DC power.

A further problem is encountered if it is desired to reactively sputter two metals at the same time to produce mixed metal oxides of controlled composition. The metals operate in different ranges of partial pressure of the reactive gas for their optimum deposition, which also changes with the power that is used, and it is difficult to operate a system with both sources operating in the desired metal sputtering mode.

This paper reports on the deposition of mixed metal oxides using a simultaneous oxidisation stage, controlled by spectral radiation from the discharge (plasma emission monitoring, or PEM), or the cathode voltage in constant-power sputtering. This is used in conjunction with movement of the sample between that source and one sputtering the other metal. The process was optimised with witness pieces admitted through an air lock into a continuously operating system. The second metal was oxidised in the unbalanced magnetron discharge of the first, i.e. a SPA process, whose sputtered metal was simultaneously converted. Power (40 kHz) was applied between the two cathodes and a DC bias used to adjust the ratio of metals in the mixed oxide. The stoichiometry was determined by the partial pressure, i.e. the PEM signal, in that chamber, the power applied and the rate of rotation.

2. The techniques

2.1. Mid-frequency AC powered magnetrons in floating mode with a DC bias

For the coating composition to be easily controlled, the amount of power (or current) received by one/both of the floating magnetrons has to be independently varied. This was achieved by DC-biasing one of these magnetrons. In most cases, the two floating magnetrons were operated at a constant AC power, using the 40-kHz supply, whereas the DC power, applied to one of the magnetrons, was varied. Such a method of combined AC and DC power application enjoys the following major advantages:

1. It paves the way to produce coatings of virtually any desired composition by simply varying the ratio of the applied DC and AC powers.
2. It retains the advantages of applying mid-frequency AC power, between two floating magnetrons.
3. It also retains the advantages of applying DC power, such as high deposition rates onto large area substrates.

The AC power supply was isolated from the DC with a capacitor and the DC from the AC with a LCL filter. Fig. 1 shows a schematic diagram of this filter. It should be emphasised, that the plasma was earthed through the chamber wall to provide the DC return path for the current. Initial experiments were carried out with two Al targets, sputtered in an Ar atmosphere. An oscilloscope was used to measure the DC potential developed on the magnetrons, relative to earth, in the following cases:
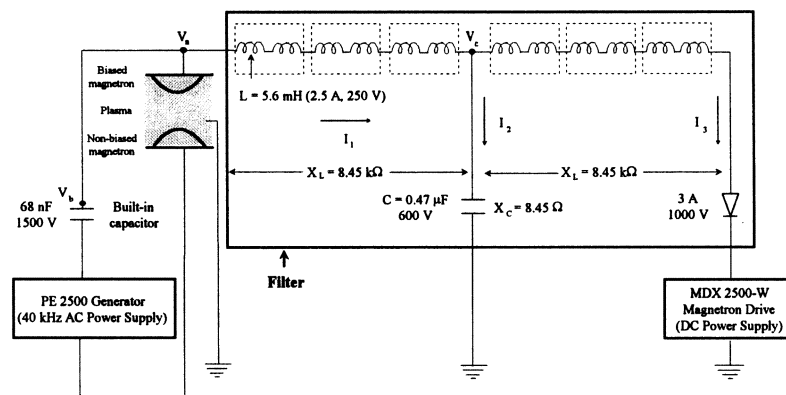
1. On one of the magnetrons when the applied power

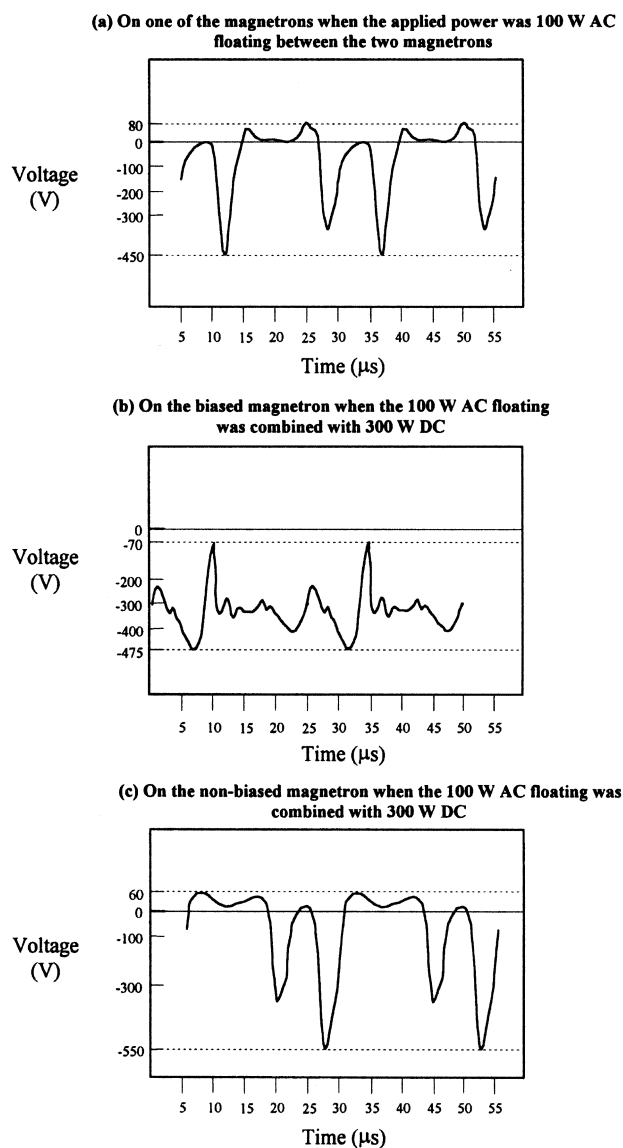Fig. 1. The filter used to protect the DC power supply from AC currents.

(a) On one of the magnetrons when the applied power was 100 W AC floating between the two magnetrons

Voltage (V)

Time (µs)

(b) On the biased magnetron when the 100 W AC floating was combined with 300 W DC

Voltage (V)

Time (µs)

(c) On the non-biased magnetron when the 100 W AC floating was combined with 300 W DC

Voltage (V)

Time (µs)

Fig. 2. A reproduction of the photographs taken from the oscilloscope for the DC potentials, relative to earth, developed on a floating, biased and non-biased Al magnetron.

was 100 W AC floating between the two magnetrons (Fig. 2a).

2. On both the biased (Fig. 2b) and the non-biased (Fig. 2c) magnetrons, when the 100-W AC floating was combined with a 300-W DC power to bias one of the magnetrons (a common case).

A similarity can be noticed between Fig. 2a,c. To understand the reason behind that, the reader is referred to Fig. 1. The capacitor shown in the AC part of the circuitry is an internal component of the output stage of the AC power supply. Its purpose is to block any DC component of current should there be any, emanating from the AC power supply, and has twofold ramifications. The first is that the current, in the AC

part of the circuit, is to be the same in both directions when a DC bias is applied. Secondly, without a DC bias, the capacitor is charged/discharged following the voltage waveform of the AC power supply. Alternatively, when a DC bias is applied to one of the magnetrons, the capacitor is charged/discharged (via the biased magnetron) following the voltage difference $V_a - V_b$, where V_a is the fixed DC voltage and V_b is the alternating AC one. This leads to a slight change in the AC current in the AC part of the circuit from that when only the AC power was applied. As a result, a slight change in the voltage of the non-biased magnetron should also occur to maintain AC current magnitude in both directions. In other words, for periods when the AC current flow is in the same direction to the DC current, the capacitor will charge due to the latter. This accumulated charge is discharged onto the biased magnetron. In order to maintain AC current magnitude in both directions, the non-biased magnetron must develop an appropriate bias, as can be noticed by comparing the positive voltage regions of Fig. 2a,c. Consequently, Fig. 2a can be regarded as a representative voltage waveform for such a circuit. Comparing Fig. 2a,c, it is suggested that the AC current (in the AC part of the circuit) is indeed approximately equal in both cases. The magnitudes in both directions are approximately equal, within the biased magnetron arrangement.

On the other hand, whenever the DC potential of the magnetron is negative with respect to the plasma potential (earth potential in this case), sputtering will occur. It is easy to see, then, from Fig. 2b, that the biased magnetron is sputtering continuously, albeit to various degrees. Fig. 2c shows that the non-biased cathode is not sputtering continuously; although it attains a potential of approximately −550 V, these periods are short compared to the 'off times', when its potential goes positive with respect to plasma potential. In summary, we have:

1. The biased magnetron is tied to DC potential. The current to it is the sum of the DC current driven from the DC power supply and the current that is driven from the AC power supply. The existence of a DC bias means that the plasma has to be earthed, by contact with the chamber walls, to allow the DC current to flow.
2. The non-biased magnetron will adjust its internal DC voltage so as the AC current flowing around the AC part of the arrangement is equal in magnitude for both current directions (i.e. to both magnetrons). This results in a constant AC power applied to each cathode, provided the target materials are identical.

2.2. Plasma emission monitoring (PEM)

This method of control has been described in detail in a previous paper [6]. In the course of this work, the plasma contained mainly the emission lines corresponding to argon, oxygen and the target material. Therefore, to control the emission line/s of one of these elements, the optical filter had to be chosen so as either the wavelength/s of light it transmitted was unique to this element, or the emission intensity at the selected wavelength/s was sufficiently higher than the corresponding ones of the other two elements.

For example, for the reactive sputter-deposition of In oxide, a band pass filter had been used for controlling on In emission line at 451.1 nm. Sufficient signals up to approximately 150 mV were obtained at applied powers of the order of 300 W. At this wavelength, there is neither an argon nor an oxygen line, sufficiently intense, to interfere with the In one. A more universal technique was required for the large number of materials investigated in this work. A high-pass filter, with a cut-off wavelength at approximately 620 nm, was successfully used to control the reactive sputter-deposition of W, V, Mo and Ti oxide. At wavelengths greater than approximately 620 nm, the intensities of the emission lines of these metals are very weak. Thus, the transmitted signal by this filter is either due to argon or oxygen-lines. The signal fell as oxygen was admitted and it is concluded that the strong signal was due to argon, and the control was carried out on the argon lines, the fall in intensity being attributed to changes in the discharge current and coupling to the components of the atmosphere as the oxygen was added. Signals up to approximately 1.5–2 V were obtained at applied powers of the order of 300 W.

2.3. Voltage control

Voltage control has been described in detail in a previous paper [6]. This method of control has been used in this work in the cases of Al, Zn, Cu and Pb when they were sputtered in an Ar/O_2 atmosphere.

Fig. 3 shows a schematic of the voltage control loop. A user connector, located on the rear panel of the Advanced Energy™ power supplies which was used in this work, provides a 0–5-V DC analogue signal representing the cathode voltage (i.e. the output voltage of the power supply). The DC signal was 0 V when the output voltage of the supply was also 0 V and it was 5 V at the full-scale output voltage of the supply. This 0–5-V DC signal was used as an input to a voltage controller. The signal was taken through two controls; one of which backs it off against another potential to provide a zero reference. The difference from this zero signal was then amplified by a variable gain amplifier to give an output ranged from 0 to 1 V. The output signal
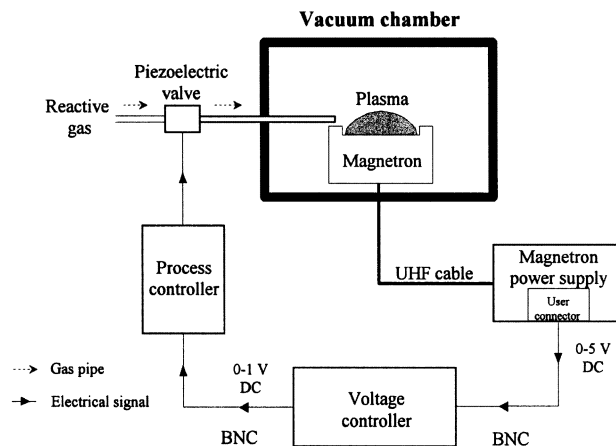

Fig. 3. Voltage control (VC) system used in controlling the reactive magnetron sputtering processes.

from the voltage controller was then applied to a standard pressure controller (process controller) which was connected to a piezoelectric control valve of a very fast response. The 'zero reference' was the signal corresponding to the voltage seen when the target was fully poisoned, the '1' was that for metal sputtering. Any intermediate degree of target poisoning (i.e. an intermediate value of cathode voltage) can be represented, in this technique, by a value of input voltage to the controller in the range 0–5 V, and a value of output voltage in the range 0–1 V. The input to the voltage controller was taken from the DC power supply, when it was used, as it represented the dominating power applied to the main magnetron relative to the floating power applied by the AC power supply. This arrangement provided better control.

2.4. Substrate condition probe

The information that was required was the ion current density to the substrate and its floating potential. In other words, the number and energy of ions that bombarded the growing films relative to the number of atoms deposited. To obtain this information, we used what we termed a 'substrate condition probe'. Fig. 4 shows a cross-sectional and a bottom view (i.e. the surface with a direct contact with the plasma) of this probe. It essentially consisted of a central cylindrical head, whose diameter was 6 mm, surrounded by a 25×37 mm guard. The guard, which was entirely isolated from the head, was utilised to minimise the plasma edge-effect from the probe head. The probe was placed in the plane of the substrate following the same procedure of placing a substrate; it was mounted in the jig, which was in turn inserted into the platen.

The I–V characteristics were then obtained by biasing the probe head. The current to the guard was excluded. Probe measurements were performed using
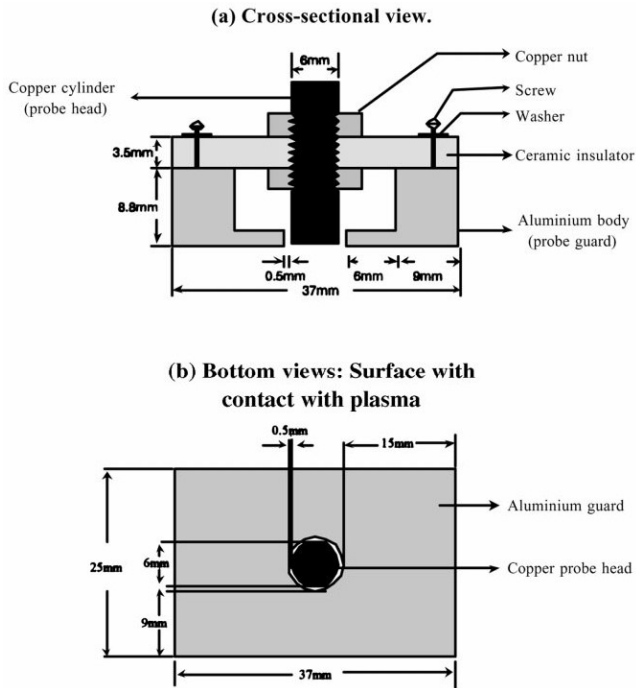
Fig. 4. A cross-sectional and a bottom view of the probe.

Fig. 6. The negative part of the I–V characteristics of the probe, at different DC powers to an In magnetron, when it was held opposite the centre of the magnetron. The curve when the probe was held opposite the erosion zone is also plotted.

In and Sn targets attached to the main and secondary magnetrons, respectively. Keeping the working pressure at 2×10^{-3} torr, two sets of experiments were carried out. The first was when the probe was held opposite to the centre of the In magnetron using different DC powers (i.e. at 100, 200 and 300 W). In addition, the characteristics of the probe when it was facing the erosion zone of the In magnetron, when the applied power was 300 W, was also plotted for comparison. The results are shown in Figs. 5 and 6. In the second set of experiments, the probe was held opposite to the centre of the In magnetron throughout. The applied powers were 50 W and 100 W AC floating between the two magnetrons, and 300 W DC combined with 100 W AC. The results are shown in Fig. 7. The following remarks can be deduced from these figures:

1. The ion-current to the probe increased with the applied DC power to the magnetron. On the other hand, at a fixed DC power (e.g. 300 W), such a current was higher when the probe was held opposite the centre of the magnetron than when it was opposite the erosion zone. Similarly, the ion-current to the probe also increased with the applied floating AC power.
2. At a fixed magnitude of power (e.g. 100 W), the ion-current to the probe was lower in the DC case than in the floating AC one. Furthermore, the ion-current to the probe in the case of the 100-W AC combined with 300-W DC was the highest (Fig. 7).
3. The floating potential of the probe was almost independent of the applied AC power and slightly dependent on the DC power. However, the order of magnitude of these floating potentials was slightly lower when DC powers were applied.

The above conclusions are in very good agreement with the results obtained by Window and Savvides [12] and the results of Glocker [8]. In addition, the ion-current and floating potential, when the probe was opposite to the erosion zone, are less than the corresponding values when the probe was opposite to the centre of
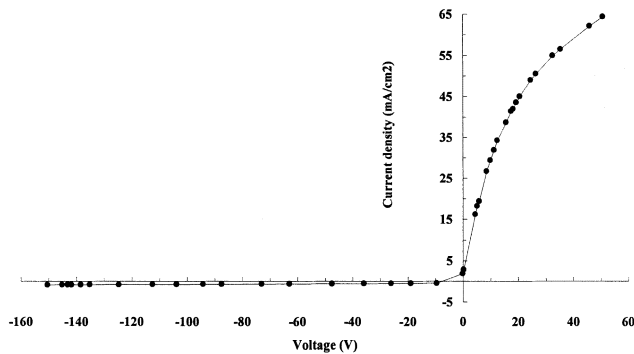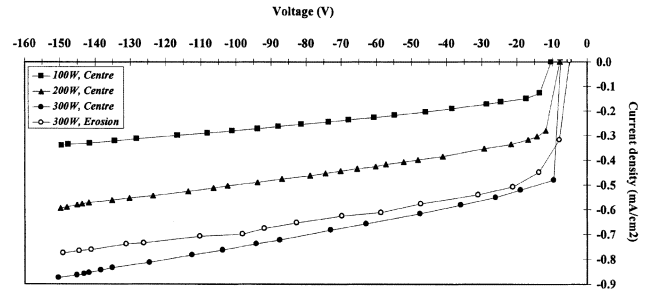

Fig. 5. The I–V characteristics of the probe when an In magnetron was held at 300 W DC and the probe was held opposite to the centre of the magnetron.
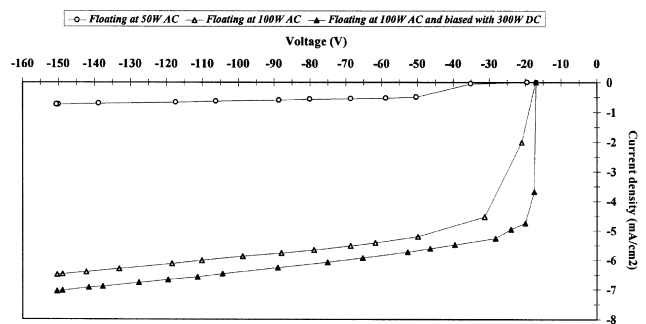

Fig. 7. The negative part of the I–V characteristics of the probe at different AC powers to a non-biased and biased floating In magnetron when the probe was held opposite the centre of the magnetron.

the magnetron under the same conditions (i.e. applied power). This result is also in good agreement with those of Howson et al. [13] and Spencer et al. [14].

It is informative to compute the arrival ratio of Ar ions to metal atoms at the substrate. It was found that this was 0.7 and the energy delivered to the substrate by ions per In atom was approximately 21 eV [1–6].

On the other hand, in the case when the applied power to the magnetron was 300 W DC combined with 100 W AC, $J_i^s = 7.1$ mA/cm^2, $V_f = -17$ V and $V_p = 0$ V (Fig. 7), where J_i^s, V_f and V_p are the ion current density to the substrate, the floating potential of the substrate and the plasma potential, respectively. Considering the case of indium oxide, which had a thickness of 152 nm, it was found that $N_i^s / N_m^s = 5.7$, where N_i^s and N_m^s are the number of ions bombarding 1 cm^2 of the substrate per second and the number of deposited metal atoms on 1 cm^2 of the substrate per second, respectively. Consequently, the energy delivered to the substrate by ions per In atom was approximately 100 eV.

Although the two magnetrons were unbalanced in the system used in this work, the measured floating potentials of the substrate were relatively low, whereas, the measured ion current densities were moderate. This could be due to the fact that target-to-substrate distance is less than the null-point of the magnetrons, which means that, at such low distance, ions cannot acquire high kinetic energies when they impinge on the substrate, with the lower floating potential that the substrates have. The small target-to-substrate distance also affects, but less severely, the ion current density, as the substrate can not collect all ions available because it is not in the way of the focused beam leaking from the cathode, rather it is in the base of that beam. The average ion densities in the AC plasma are approximately four times that of the DC plasma. This last difference, between the AC and the DC plasmas is significant. According to optical emission measurements, the plasma extinguishes on each half-cycle and has to be reignited. The increase in ion densities in the AC plasma was attributed to target voltage spikes during the reignition of the plasma on each half-cycle, as it is evident on the negative-going part of each cycle. Such spikes cause rapid electron acceleration in the pre-sheath region leading to significantly more efficient ionisation of gas and hence much higher plasma bombardment.

3. Experimental details

3.1. The sputtering system

The chamber comprised a 42-cm diameter stainless steel chamber, 12-cm deep internally, giving a short pump down time with the turbomolecular pump, backed by a two-stage rotary pump, compared with conventional bell-jar systems [3]. The chamber base accommodated two identical magnetrons. The magnetron, which had both the oxygen inlet to the chamber and the optical fibre input tip of PEM control loop attached to its pod will be, henceforth, called the 'main magnetron'. The other magnetron was connected to the argon inlet to the chamber.

An axially mounted aluminium platen was located above the magnetron cathode surfaces, and it was onto this platen, which was electrically isolated, the substrates were loaded from the airlock allowing a target-to-substrate distance of approximately 40 mm. The centrally oriented metal shaft was attached to the platen so that it could be rotated around this axis with a DC motor at a rotation speed of up to 60 rev./min.

The partial pressure of the sputtering gas, argon, was produced through a mass flow controller balanced by the vacuum pumping and measured with the system pirani.

For the admission of reactive gas a solenoid valve was replaced by a piezoelectric valve, having a faster response in order to cope with much faster changes in the desired supply of reactive gas required to maintain a certain cathode status, compared with that of inert gas. This was controlled to produce a pre-determined optical emission signal or cathode potential in much the same way as is used to control pressure. In addition, the total distance between the reactive gas pipe exit in the chamber and the piezoelectric valve was minimised to help reducing the time constant of the pipe. These modifications, allied with the pipe outlet being very close to the target in the very confined volume provided by the gettering enabled very efficient control of the reactive deposition processes to be obtained.

3.2. The airlock system

The system was designed so that the magnetrons could be operated continuously during the changing of substrates. We have found this to be of prime importance for iterative reactive processing, in which the partial pressure of the reactive gas is varied gradually until the desired film properties are attained. In order that this could be done the system was airlocked, that is, the main deposition chamber always remained in operation whilst the samples could be loaded/unloaded via a separately pumped airlock. The airlock was 10 cm in diameter and 4.6 cm deep, had a 0.361 l volume, and could typically be evacuated from atmosphere to approximately 40 mtorr in approximately 2 min, via two-stage rotary pump.

Samples were mounted singly in a jig, which was then attached to the end of a loading arm, which was moved

linearly through double Wilson-type vacuum seals, mounted off axis (2.2 cm from the centre) in the perspex window plate, which allow visual location of the substrate.

4. Optical measurements

4.1. Calculations of refractive indices from reflectance spectra

In this section, the case of transparent non-absorbing films deposited on transparent substrates will be considered. It should be mentioned first that the wavelength λ of the incident light is chosen so that it is comparable to the film thickness d_{film} to allow interference effects to occur [15].

The maximum and minimum reflectance of a thin film on an infinitely thick substrate are given by:

$$R_{max} = \left(\frac{n_{film}^2 - n_{amb} n_{subs}}{n_{film}^2 + n_{amb} n_{subs}} \right)^2 \quad (1)$$

$$R_{min} = \left(\frac{n_{subs} - n_{amb}}{n_{subs} + n_{amb}} \right)^2 \quad (2)$$

where R_{max}, R_{min}, n_{film}, n_{subs} and n_{amb} are a reflectance maximum, reflectance minimum, the refractive index of the thin film, the refractive index of the substrate and the refractive index of the ambient medium, respectively. By solving Eq. (1) for n_{film}, we get:

$$n_{film} = \left(n_{amb} n_{subs} \frac{1 + \sqrt{R_{max}}}{1 - \sqrt{R_{max}}} \right)^{1/2} \quad (3)$$

The relative precision of n_{film} is given by

$$\frac{\Delta n_{film}}{n_{film}} = \frac{\sqrt{R_{max}}}{2(1 - R_{max})} \frac{\Delta R_{max}}{R_{max}} \quad (4)$$

For example, if $R_{max} = 36\%$, it is then sufficient to measure R_{max} to an accuracy of approximately 2% (i.e. $\Delta R_{max} = 0.7\%$) so that the relative error for n_{film} is not larger than 1%.

In this work, films were deposited on glass substrates with $n_{subs} = 1.525$ and the spectrophotometric measurements were carried out in air (i.e. $n_{amb} = 1$).

Transmittance and reflectance spectra of transparent films, produced in this work, were measured using a Hitachi U-2000 double-beam spectrophotometer with a simple reflection attachment, which allowed comparison of the sample with freshly prepared aluminium
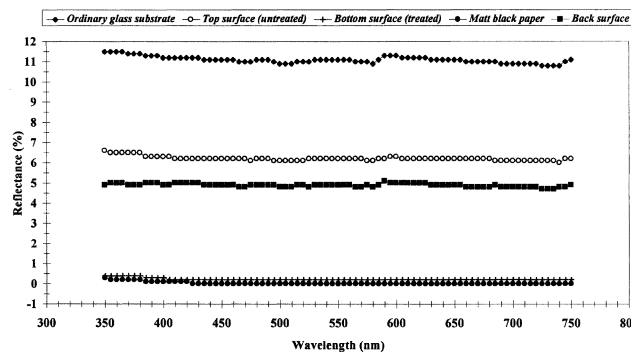

Fig. 8. Reference spectra of uncoated glass substrates in different cases. The reflectance spectrum of matt black paper is included for comparison.

coating. In spectrophotometric measurements carried out in this work, both transmittance and reflectance spectra were measured in the spectral range 350–750 nm with a scanning speed of 400 nm/min.

In order to obtain values for the absolute reflection coefficients that were required, it was necessary to make corrections of the measured reflectance spectra of the deposited films. The corrections involved:

1. Measuring the reflectance spectrum of the bottom surface of an uncoated glass substrate in order to subtract it from the measured values of reflectance. This was achieved by treating the bottom surface of an uncoated glass substrate with emery paper so virtually eliminating reflection from it (Fig. 8). The reflectance spectra of the untreated (or top) surface and that of an ordinary glass substrate were then measured. The reflectance spectrum of the back surface was obtained by subtracting the reflectance values of the top surface from those of the ordinary substrate, and was averaged to be 5%.
2. Measuring the reflectance spectrum of a single crystal silicon wafer and comparing it with a calculated one [16] to derive a correction curve of the measured reflectance in order to obtain the absolute reflectance of the coatings (Fig. 9). The correction ratio was, on average, 0.76.

Thus, the relation between the measured reflectance, R^{measur}, and the actual one, R, is

$$R \approx 0.76(R^{measur} - 5\%) \quad (5)$$

or

$$R \approx 0.76 R^{measur} - 4\% \quad (6)$$

As a result, if R_{max}^{measur} is the measured value of a reflectance maximum, the corresponding actual value, R_{max}, is given by
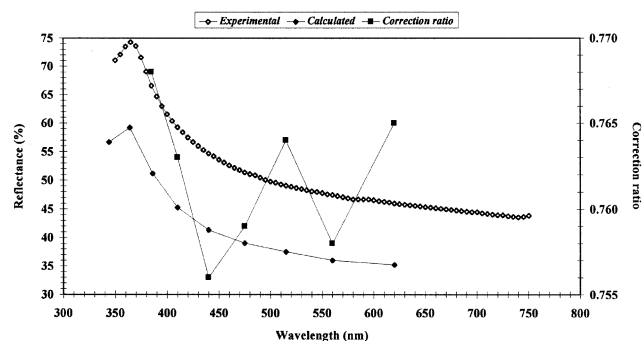
Fig. 9. Calculated and experimental reflectance spectra of a single crystal silicon wafer. Also shown is the correction ratio as a function of wavelength. Data of the calculated curve are from [16].

$$R_{\max} \approx 0.76 R_{\max}^{\mathrm{measur}} - 4\% \qquad (7)$$

Thus, by substituting the value of $R_{\max}$:

$$n_{\mathrm{film}} = \left(1.525 \frac{1 + \sqrt{0.76 R_{\max}^{\mathrm{measur}} - 0.04}}{1 - \sqrt{0.76 R_{\max}^{\mathrm{measur}} - 0.04}} \right)^{1/2} \qquad (8)$$

Instead of ellipsometry, Eq. (8) was used to calculate refractive indices of films produced in the course of this work, for the following reasons:

1. It is independent of optical thickness of coatings and consequently gives consistent results for variable optical thickness.
2. The possibility of obtaining refractive indices over many wavelengths rather than at 632.8 nm using the ellipsometer that was available.
3. The ratio of the area of light beam of the spectrophotometer (~ 10.8 mm^2) and that of the laser beam of the ellipsometer (~ 0.8 mm^2) is approximately 14. This gives better integration over the coated area of the substrate.

4.2. Calculations of thickness from reflectance spectra using interference methods

After calculating n_{film}, using Eq. (8) the film thickness could be calculated using equations $n_{\mathrm{film}} d_{\mathrm{film}} = (2k + 1) \frac{\lambda_{\max}}{4}$ and $n_{\mathrm{film}} d_{\mathrm{film}} = k \frac{\lambda_{\min}}{2}$, where $\lambda_{\max}$ is a wavelength at which a reflectance maximum occurs and $\lambda_{\min}$ is a wavelength at which a reflectance minimum occurs. The calculation procedure depended on the shape of the reflectance spectrum of interest.

If there were two consecutive maxima in the scanned spectral range, then for the first maximum $4 n_{\mathrm{film}} d_{\mathrm{film}} = (2k + 1) \lambda_{\max_1}$ and that for the second maximum is $4 n_{\mathrm{film}} d_{\mathrm{film}} = [2(k - 1) + 1] \lambda_{\max_2}$. By solving these two equations, it is found that

$$d_{\mathrm{film}} = \left| \frac{\lambda_{\max_1} \lambda_{\max_2}}{2 n_{\mathrm{film}} (\lambda_{\max_2} - \lambda_{\max_1})} \right| \qquad (9)$$

Eq. (9) is also valid in the case of two consecutive minima. The problem of this equation is that it ignores changes of n_{film} with wavelength. However, it was considered to be sufficiently accurate for the estimation of d_{film} for the purpose of this work, especially in the relatively narrow range of wavelength studied where variations in n_{film} were not expected to be so significant.

Finally, it should be indicated that the results of the thickness measurements were satisfactorily consistent in the course of this work.

5. Results

5.1. Aluminium oxides

The system was established using aluminium cathodes in both magnetrons. Aluminium oxide is a very insulating oxide with a high secondary electron emission coefficient, which leads to extreme arcing if DC reactive sputtering is attempted.

In this work, Al_2O_3 films were prepared using the mid-frequency AC powered magnetrons technique. The main and secondary targets were both Al and the two magnetrons were operated in the floating mode at $P_{Al \leftrightarrow Al}^{AC} = 1$ kW. Substrates were held static over the main magnetron. In this case, no incorporation of an alloying material was required. Voltage control on the main Al magnetron was used. The percentage of aluminium magnetron voltage set point, $Al_{vc}^{\%}$, was gradually decreased and a film was deposited and characterised at each value of $Al_{vc}^{\%}$. The deposition time was 3 min. Fig. 10 shows the dependence of transmittance at 550 nm, T_{550}, of the visibly transparent Al_2O_3 films, and the corresponding deposition rate, on $Al_{vc}^{\%}$. Obviously, films of higher T_{550} are deposited at lower rates. The percentage of Al magnetron voltage set point, and the corresponding O_2 flow rate, at which the best Al_2O_3 film occurred (i.e. the one of the highest transmittance and deposition rate) were 73.7% and 3.6 sccm, respectively. The transmittance at 550 nm, refractive index and deposition rate of this film were 89.5%, 1.67 and 2.02 nm/s, respectively. Clearly, such a result is comparable with the best reported results [9,17,18], taking into account that the applied power in this work was only 1 kW. Fig. 11 shows the transmittance and reflectance spectra of the best Al_2O_3 film. Finally, it is worth mentioning that, in addition to glass, aluminium oxide films have also been deposited, using this technique, on stainless steel and single crystal silicon substrates for extended periods of time (up to 45 min) and at high rates without any sign of arcing.

5.2. Mixed insulating oxides

Finally, a large number of oxide films of Mo, W, V, Pb, Ti, Sn and Cu doped with dopants such as Zn, Sn, Ti, Nb, Ta, Mo or Bi have been deposited, at different combinations of powers and at different stoichiometries, and characterised. They were initially investigated for conductivity. Although the transparent films were insulating under the deposition conditions and procedures followed (i.e. unintentional heating or biasing of substrates and no post-deposition heat treatment), their optical properties (e.g. a very wide range of refractive indices) are of great interest in optical applications.

Table 1 summarises the preparation conditions and the optical properties of some of the transparent insulating oxide films prepared in this work, where P_{Cu}^{DC}, P_W^{DC}, P_V^{DC}, P_{Mo}^{DC} and P_{Pb}^{DC} are the DC biasing powers applied to the floating Cu, W, V, Mo and Pb magnetrons, respectively, and $Cu_{vc}^{\%}$ and $Pb_{vc}^{\%}$ are the percentages of metallic Cu and Pb magnetrons voltages set-points (i.e. the occurrence), respectively. The floating AC power and deposition time were 100 W and 6 min, respectively, throughout.

6. Conclusion

According to the above discussion, the deposition technique, employed in the course of this work, enjoys the following major advantages

1. Substrate rotation enhances atomic level mixing of the film constituents. The stoichiometry of the film is controlled by PEM or voltage control, on one magnetron, and dopants are added by sputtering from the other magnetron. This means that the former magnetron serves two purposes; the first is to sputter metal and oxidise it, and the second purpose is to oxidise the metal sputtered from the other magnetron.
2. The combination of DC and mid-frequency AC
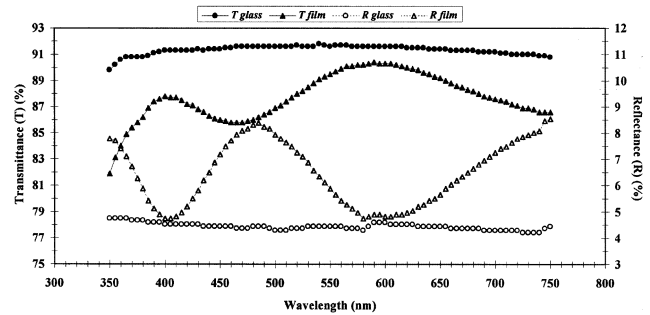
Fig. 11. Transmittance and reflectance spectra of the best transparent Al oxide film which occurred at 73.7% of Al magnetron voltage set-point. The floating AC power was 1 kW. The relevant spectra of an uncoated glass substrate are also plotted.

power in a novel way, using a filter to protect the DC power supply from the AC one (or the independently DC powered magnetrons method), permits the composition of the produced films to be easily and independently manipulated by varying the magnitude of power applied to each magnetron. As a result, this system is able to obtain a sputter-deposited coating of an alloy or multi-element compound which is either difficult or impossible to be formed from a single target.

3. Depending on the materials involved, the use of very fast feedback methods, to automatically control the admission rate of the reactive gas (e.g. oxygen) into the sputtering chamber (i.e. PEM and voltage control), allows the stoichiometry of the deposited films to be independently controlled. The very efficient control of the admission rate of oxygen also allows the deposition rate of reactively sputtered films to be high.

4. The use of an airlocked system allows the implementation of an iterative deposition process to vary coating stoichiometry and composition. Hence, information regarding different composition and stoichiometry can be attained rapidly without cathode acquisition or preparation.

5. The system, described in this work, is superior to the dual magnetron technique described by Lewin and Howson [19] where two concentric cathode annuli of different materials (with separate magnetic fields) comprise one magnetron device in that the two sources sputter independently of each other. This permits variable compositions to be selected only to a limited extent in a reactive environment, the limit being reached when differential poisoning of the two cathode materials dominates. Clearly, precise stoichiometry control also suffers from this problem as a direct result of the close proximity of the cathode.

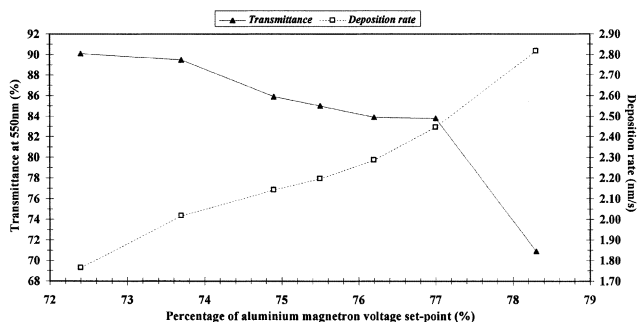6. The use of mid-frequency (i.e. 40 kHz) AC power in the floating mode secures periodical effective

Fig. 10. Transmittance at 550 nm and the corresponding deposition rate vs. the percentage of aluminium magnetron voltage set-point of visibly transparent films of aluminium oxide. The floating AC power between the two Al magnetrons was 1 kW.

Table 1
A summary of the preparation conditions and optical properties of some of the transparent insulating oxide films prepared in this work[a]

Oxide	DC bias (W)	Occurrence (%)	n_{film}	T_{550} (%)	Deposition rate (nm/s)
Cu–Sn	$P_{\text{Cu}}^{\text{DC}} = 300$	$\text{Cu}_{\text{vc}}^{\%} = 30.8$	1.92	67.7	0.80
Mo–Nb	$P_{\text{Mo}}^{\text{DC}} = 150$	$\text{Ar}_{\text{pem}}^{\%} = 53.9$	2.24	72.3	0.36
Mo–Nb	$P_{\text{Mo}}^{\text{DC}} = 300$	$\text{Ar}_{\text{pem}}^{\%} = 49.3$	1.96	91.9	0.41
Mo–Nb	$P_{\text{Mo}}^{\text{DC}} = 450$	$\text{Ar}_{\text{pem}}^{\%} = 46.3$	1.93	91.9	0.44
Mo–Sn	$P_{\text{Mo}}^{\text{DC}} = 100$	$\text{Ar}_{\text{pem}}^{\%} = 54.0$	2.00	81.4	0.30
Mo–Sn	$P_{\text{Mo}}^{\text{DC}} = 300$	$\text{Ar}_{\text{pem}}^{\%} = 51.4$	2.17	90.8	0.37
Mo–Ta	$P_{\text{Mo}}^{\text{DC}} = 450$	$\text{Ar}_{\text{pem}}^{\%} = 45.9$	2.09	90.9	0.42
Pb	$P_{\text{Pb}}^{\text{DC}} = 400$	$\text{Pb}_{\text{vc}}^{\%} = 54.0$	2.46	74.2	1.25
Pb–Bi	$P_{\text{Pb}}^{\text{DC}} = 100$	$\text{Pb}_{\text{vc}}^{\%} = 52.0$	2.44	80.9	0.84
Pb–Bi	$P_{\text{Pb}}^{\text{DC}} = 300$	$\text{Pb}_{\text{vc}}^{\%} = 42.8$	2.40	88.4	1.28
Pb–Bi	$P_{\text{Pb}}^{\text{DC}} = 400$	$\text{Pb}_{\text{vc}}^{\%} = 41.4$	2.39	84.0	1.55
Ti	$P_{\text{Ti}}^{\text{DC}} = 400$	$\text{Ar}_{\text{pem}}^{\%} = 65.1$	2.63	80.1	0.05
Ti–Nb	$P_{\text{Ti}}^{\text{DC}} = 400$	$\text{Ar}_{\text{pem}}^{\%} = 69.1$	2.60	67.1	0.09
Ti–Ta	$P_{\text{Ti}}^{\text{DC}} = 400$	$\text{Ar}_{\text{pem}}^{\%} = 67.7$	2.28	69.9	0.17
V–Mo	$P_{\text{V}}^{\text{DC}} = 200$	$\text{Ar}_{\text{pem}}^{\%} = 68.9$	1.80	77.9	0.52
V–Mo	$P_{\text{V}}^{\text{DC}} = 300$	$\text{Ar}_{\text{pem}}^{\%} = 65.6$	1.79	81.4	0.48
W	$P_{\text{W}}^{\text{DC}} = 400$	$\text{Ar}_{\text{pem}}^{\%} = 51.6$	2.23	76.4	0.76
W–Mo	$P_{\text{W}}^{\text{DC}} = 150$	$\text{Ar}_{\text{pem}}^{\%} = 53.8$	2.29	91.2	0.34
W–Mo	$P_{\text{W}}^{\text{DC}} = 450$	$\text{Ar}_{\text{pem}}^{\%} = 50.0$	2.20	87.0	0.71
W–Nb	$P_{\text{W}}^{\text{DC}} = 200$	$\text{Ar}_{\text{pem}}^{\%} = 62.1$	2.29	90.8	0.38
W–Nb	$P_{\text{W}}^{\text{DC}} = 350$	$\text{Ar}_{\text{pem}}^{\%} = 51.9$	2.21	84.8	0.70
W–Nb	$P_{\text{W}}^{\text{DC}} = 400$	$\text{Ar}_{\text{pem}}^{\%} = 55.1$	2.14	74.0	1.37
W–Sn	$P_{\text{W}}^{\text{DC}} = 100$	$\text{Ar}_{\text{pem}}^{\%} = 51.9$	2.14	91.5	0.36
W–Ta	$P_{\text{W}}^{\text{DC}} = 200$	$\text{Ar}_{\text{pem}}^{\%} = 60.6$	2.29	78.1	0.59
W–Ta	$P_{\text{W}}^{\text{DC}} = 400$	$\text{Ar}_{\text{pem}}^{\%} = 56.8$	2.21	70.7	0.83
W–Ta	$P_{\text{W}}^{\text{DC}} = 600$	$\text{Ar}_{\text{pem}}^{\%} = 56.3$	2.12	86.3	1.05
W–Ti	$P_{\text{W}}^{\text{DC}} = 150$	$\text{Ar}_{\text{pem}}^{\%} = 55.6$	2.31	91.1	0.35
W–Ti	$P_{\text{W}}^{\text{DC}} = 450$	$\text{Ar}_{\text{pem}}^{\%} = 52.0$	2.24	87.9	0.64

[a] The floating AC power was 100 W throughout.

discharging of the insulating layer, due to the symmetrical operation of the electrodes. This allows the reactive sputtering process to be arc-free [9], and hence, eliminating the undesired effects of arcing in reactive sputtering such as driving the process to become unstable, creating defects in the films and reducing the target lifetime. Consequently, the defect density in insulating films is reduced by orders of magnitude [11] in comparison with the DC technique.

7. The well-defined DC conducting anode allows the sputtering process to have long-term stability, at a given set point. In addition, the high deposition rates obtained are comparable with those of the DC technique [7,9].

8. Unlike the additional complexity of the RF technique, the coupling of the AC power to the cathodes, in the frequency range used, is simple. Consequently, the AC technique can be easily adopted for sputtering from larger area cathodes [9]. On the other hand, the AC plasma used with an unbalanced magnetron leads to higher density plasma and increased bombardment of the growing insulating films with ions.

9. This technique opens the door wide for investigating virtually all potentially promising thin films (e.g. hard coatings, semiconducting films, superconducting films, etc.).

References

[1] N. Danson, I. Safi, G.W. Hall, R.P. Howson, Surf. Coat. Technol. 99 (1998) 147–160.
[2] R.P. Howson, N. Danson, I. Safi, Thin Solid Films 351 (1999) 32–36.

[3] R.P. Howson, I. Safi, G.W. Hall, N. Danson, Nucl. Instrum. Methods Phys. Res. B 121 (1997) 96–101.

[4] I. Safi, N. Danson, R.P. Howson, Surf. Coat. Technol. 99 (1998) 33–41.

[5] I. Safi, R.P. Howson, Thin Solid Films 343-44 (1999) 115–118.

[6] I. Safi, Surf. Coat. Technol. 127 (2-3) (2000) 203–219.

[7] J. Szczyrbowski, C. Braatz, SPIE 1727 (1992) 122–136.

[8] D.A. Glocker, J. Vac. Sci. Technol. A 11 (6) (1993) 2989–2993.

[9] M. Scherer, J. Schmitt, R. Latz, M. Schanz, J. Vac. Sci. Technol. A 10 (4) (1992) 1772–1776.

[10] G. Este, W.D. Westwood, J. Vac. Sci. Technol. A 6 (3) (1988) 1845–1848.

[11] S. Schiller, K. Goedicke, J. Reschke, V. Kirchhoff, S. Schneider, F. Milde, Surf. Coat. Technol. 61 (1993) 331–337.

[12] B. Window, N. Savvides, J. Vac. Sci. Technol. A 4 (3) (1986) 453–456.

[13] R.P. Howson, H.A. Ja'Fer, A.G. Spencer, Thin Solid Films 193-94 (1990) 127–137.

[14] A.G. Spencer, K. Oka, R.P. Howson, R.W. Lewin, Vacuum 38 (1988) 857–859.

[15] F. Abeles, in: E. Wolf (Ed.), Progress in Optics, II, North-Holland Publishing Company, Amsterdam, 1963, pp. 249–288.

[16] D.E. Gray, American Institute of Physics Handbook, McGraw-Hill Book Company, New York, 1972.

[17] M. Scherer, P. Wirz, Thin Solid Films 119 (1984) 203–209.

[18] P.J. Clarke, J. Vac. Sci. Technol. A 12 (2) (1994) 594–597.

[19] R.W. Lewin, R.P. Howson, Proc. 6th Int. Conf. on Ion and Plasma Assisted Techniques, Brighton, UK, (1987) pp. 464–469.